Two-dimensional quantum Heisenberg antiferromagnet: Effective-Hamiltonian approach to the thermodynamics

Alessandro Cuccoli* and Valerio Tognetti†
Dipartimento di Fisica dell'Università di Firenze and Istituto Nazionale di Fisica della Materia (INFM), Largo E. Fermi 2, I-50125 Firenze, Italy

Ruggero Vaia‡
Istituto di Elettronica Quantistica del Consiglio Nazionale delle Ricerche, via Panciatichi 56/30, I-50127 Firenze, Italy and Istituto Nazionale di Fisica della Materia (INFM), Largo E. Fermi 2, I-50125 Firenze, Italy

Paola Verrucchi§
Istituto di Elettronica Quantistica del Consiglio Nazionale delle Ricerche, via Panciatichi 56/30, I-50127 Firenze, Italy and ISIS Facility, Rutherford Appleton Laboratory, Chilton, Didcot, Oxfordshire OX11 0QX, United Kingdom
(Received 28 May 1997; revised manuscript received 1 August 1997)

In this paper we present an extensive study of the thermodynamic properties of the two-dimensional quantum Heisenberg antiferromagnet on the square lattice; the problem is tackled by the pure-quantum self-consistent harmonic approximation, previously applied to quantum spin systems with easy-plane anisotropies, modeled to fit the peculiar features of an isotropic system. Internal energy, specific heat, correlation functions, staggered susceptibility, and correlation length are shown for different values of the spin, and compared with the available high-temperature expansion and quantum Monte Carlo results, as well as with the available experimental data. [S0163-1829(97)01846-8]

I. INTRODUCTION

The fully isotropic Heisenberg model may well be considered the cornerstone of modern theory of magnetic systems; the reason for such an important role is the simple structure of this model's Hamiltonian, whose high symmetry is responsible for most of its peculiar features. Recent years have seen a growing interest in the specific case of the two-dimensional quantum Heisenberg antiferromagnet (2DQHAF) on the square lattice, due both to its theoretically challenging properties and to its being the best candidate for modeling the magnetic behavior of the parent compounds of some high-T_c superconductors.[1,2]

As for the theory, the 2DQHAF cannot exhibit long-range order (LRO) for $T>0$ because of its being a two-dimensional model with a continuous symmetry (Mermin and Wagner theorem[3]); the study of the finite temperature paramagnetic phase is hence a matter of understanding what kind of disorder one is dealing with, i.e., what kind of correlation exists amongst magnetic moments on different sites. At $T=0$ quantum fluctuations make the system change from the classical-like Néel state to a ground state that can be rigorously proven[4] to be ordered for $S\geqslant 1$; for $S=1/2$ the situation is not clear yet, although more or less direct evidences for an ordered ground state, even in this extreme quantum case, can be drawn from many different studies (for a review, see, for instance, Ref. 5), including the present one (see also Ref. 6).

The experimental activity stems from the existence of several real compounds whose crystal structure is such that the magnetic ions form parallel planes and interact strongly only if belonging to the same plane. As a consequence of such structure, their magnetic behavior is indeed two-dimensional down to those low temperatures where the weak interplane interaction becomes relevant, driving the system towards a three-dimensional ordered phase; an antiferromagnetic Heisenberg interaction and a small spin value make these compounds 2DQHAF's. This is indeed the case of high-T_c superconductors of the La_2CuO_4 or $Sr_2CuO_2Cl_2$ family ($S=1/2$), of other magnets such as the $S=1$ La_2NiO_4 and K_2NiF_4, and the $S=5/2$ Rb_2MnF_4. The interplane interaction in these compounds is several orders of magnitude smaller than the intraplane one, thus offering a large temperature region where the two-dimensional behavior can be safely studied. Furthermore, their having different values of the spin allows a meaningful analysis of the spin dependence of the thermodynamic properties, which is essential if the interplay between thermal and quantum fluctuations is to be clarified.

In order to go beyond the very first treatments (mainly, mean field theory and spin wave theory), that are mostly not satisfactory in coping with its strong nonlinearity, the QHAF has been tackled by the field theory of the quantum nonlinear σ model (QNLσM).[7–9] Nevertheless, the approximations needed to reduce the actual spin model to the related field theory are drastic, as they usually approximate the essential features of magnetic systems in solid state physics, i.e., discreteness, strong nonlinearity of the Hamiltonian, and appearance of the angular momentum operators (that is, in a classical-like language, sphericity of the phase space). This inadequacy becomes more evident when experimental data are available and a quantitative comparison with theoretical predictions is attempted; realistic spin models and more refined methods must then be used, and the number of fit parameters minimized to let the real compounds drive the overall comprehension of the problem. Indeed, despite the

success in explaining some of the early experimental data, the QNLσM approach does not lead to a satisfactory understanding of the problem when higher values of the spin and higher temperatures are to be considered.[10]

This work follows a previous paper,[6] and, together with the latter, it is our attempt to move forward studying the finite temperature properties of the 2DQHAF by the effective Hamiltonian method based on the pure-quantum self-consistent harmonic approximation (PQSCHA) as developed in Ref. 11; we report here on the detailed derivation of the effective spin Hamiltonian and more results are shown as temperature and spin value are varied, together with experimental data,[12–15] classical[16,17] and quantum Monte Carlo[18,19] (MC) simulations, and high-temperature expansion[10] (HTE) results. No best-fit procedure is involved in the comparison with the experimental data, as we just need to know the spin model, which is unambiguously defined, in the case of the QHAF on the square lattice, once the values of the spin and of the exchange integral are given. The agreement we find with the available data, together with the clarity of our approach, allows us to draw a comprehensive picture of the subject, including both the analysis of the 2DQHAF behavior and the discussion of previous approaches used for the same purpose.

In Sec. II we introduce the 2DQHAF model and briefly describe the problems encountered by alternative approaches. In Sec. III the effective Hamiltonian method is described, and the approximations involved in this specific implementation are discussed; the effects of quantum fluctuations on the physics of the 2DQHAF are then analyzed in terms of the quantum renormalizations introduced by the PQSCHA. Sections IV and V contain our results for the thermodynamic properties (internal energy, specific heat, correlation functions, correlation length, and staggered susceptibility) compared with MC and HTE results, as well as with the experimental data. Conclusions are drawn in Sec. VI.

II. THE QUANTUM HEISENBERG ANTIFERROMAGNET

The two-dimensional quantum Heisenberg Antiferromagnet is described by the Hamiltonian

$$\hat{\mathcal{H}} = \frac{J}{2} \sum_{\mathbf{i},\mathbf{d}} \hat{\mathbf{S}}_{\mathbf{i}} \cdot \hat{\mathbf{S}}_{\mathbf{i}+\mathbf{d}}, \tag{1}$$

where J is positive and the quantum spin operators $\hat{\mathbf{S}}_{\mathbf{i}}$ satisfy $|\hat{\mathbf{S}}_{\mathbf{i}}|^2 = S(S+1)$. The index $\mathbf{i} \equiv (i_1, i_2)$ runs over the sites of a square lattice, and $\mathbf{d}$ represents the displacements of the four nearest neighbors of each site, $(\pm 1, 0)$ and $(0, \pm 1)$.

The most important feature of this model is the $O(3)$ symmetry of its Hamiltonian, implying no spontaneously broken symmetry for $T > 0$: the system does not support LRO at finite temperature and the standard spin-wave theory consequently produces unphysical results. The existence of local alignment directions, due to the persistence of strong short-range order up to high temperatures, makes possible the definition of a properly modified spin-wave theory[20] whose results are remarkably good. However, spin-wave theory remains quite an inadequate tool to study the thermodynamics of the 2DQHAF and this indeed stimulated several authors to search for alternative theories.

It is useful to see how disorder develops in the model described by Eq. (1) when temperature is switched on: the ground state, hereafter *assumed ordered* for any spin value, becomes unstable because of long-wavelength excitations that gradually flip the spins as one moves far from the chosen origin of the lattice; their energy is small and they do not disturb the *local* order of the system. They have a classical character in that their contribution to the thermodynamics is almost the same in both the classical and the quantum case. What makes the latter different is the additional local disorder introduced by the short-range purely quantum fluctuations, whose renormalizing effect decreases as temperature increases.

The 2DQHAF model (1) has been studied by several authors in terms of the QNLσM field theory, involving a three-component vector field $\mathbf{\Omega}$ with the constraint $|\mathbf{\Omega}| = 1$ and spatial integrations subjected to a short-distance cutoff Λ^{-1}. The model depends on two parameters: the bare *spin-stiffness* ρ_S^0 and the bare *spin-wave velocity* c_0; the coupling constant turns out to be $g_0 = c_0 \Lambda / \rho_S^0$. Despite their names, the parameters ρ_S^0 and c_0 are *not* directly related with those (J and S) defining the 2DQHAF: this relation is indeed the weakest point of the QNLσM approach.

A first link between the two models was established by Haldane and Affleck[7] under a large-S condition, i.e., in the semiclassical limit. Their mapping gives Λ, ρ_S, and c_0 as a^{-1}, JS^2, and $2\sqrt{2}JSa$, respectively (a is the lattice spacing); it follows that $g_0 = 2\sqrt{2}S^{-1}$, which means that the semiclassical limit of the spin model ($S \gg 1$) corresponds to the weak coupling regime of the field theory ($g_0 \ll 1$). The validity of this approach when studying real compounds is more than questionable, and Haldane's suggestion of replacing S by $\sqrt{S(S+1)}$ does not solve the problem.

The way Chakravarty, Halperin, and Nelson (CHN)[8] connected the two models has greater generality. They used symmetry arguments to show that the long-wavelength physics of the QHAF must be the same of that of the QNLσM, a result that holds regardless of the spin value. However, they could not define the field theory parameters in terms of those of the spin system; therefore the spin stiffness and spin wave velocity are just phenomenological fitting parameters to be determined from either experiments or simulations.

The analysis carried out by CHN on the QNLσM leads to the characterization of three different regimes, called quantum disordered, quantum critical (QCR), and renormalized classical (RCR), the most striking difference amongst them being the temperature dependence of the spin correlations. If g_0 is such as to guarantee LRO at $T = 0$, the QNLσM is in the RCR and its long-wavelength (i.e., low-temperature) physics is that of the classical model with parameters renormalized by quantum fluctuations ($\rho_S^0 \to \rho_S$, $c_0 \to c$) and a short-wavelength cutoff of order $\alpha \equiv c/T$. As far as the correlation length ξ is concerned, the famous low-temperature two-loop result for the renormalized classical regime is

$$\xi_{\mathrm{CHN}} = C_\xi \left(\frac{c}{2\pi\rho_S} \right) \exp(2\pi\rho_S / T), \tag{2}$$

where C_ξ is a nonuniversal coefficient. Hasenfratz and Niedermayer[9] have subsequently calculated the leading cor-

rection in $T/2\pi\rho_S$ to Eq. (2), and also found the coefficient $C_\xi = ea/8$, so that

$$\xi_{\mathrm{HN}} = \xi_{\mathrm{CHN}}\left[1 - \frac{T}{4\pi\rho_S} + O\left(\frac{T}{2\pi\rho_S}\right)^2\right]; \tag{3}$$

although Eq. (3) extends the temperature region where Eq. (2) can be used, both of them do not work for intermediate or high temperature. The fact that the low-temperature experimental results for $S=1/2$ two-dimensional magnetic compounds can be fitted by those of a 2DQNLσM in the renormalized classical regime, has led to assert that the ground state of the 2DQHAF is ordered also in the $S=1/2$ case.

The results by CHN are of great general value and have been extensively used to understand the $S=1/2$ experimental data, but their approach has several substantial drawbacks for that purpose. First of all, for precisely given S and J of the real compound, the fundamental parameters ρ_S and c remain unknown; the necessary best fit procedure involved in their determination introduces a substantial uncertainty in the whole of the work. Secondly, the restriction to low temperatures cannot be avoided, thus making the HTE technique, extensively used by Elstner *et al.*,[10] of great help and importance in this framework. Finally, things get worse for higher values of the spin, as has been recently pointed out by Elstner *et al.*;[10] further adjustments of the fit parameters are necessary to reproduce the experimental data[12] and the dependence of ξ upon S cannot be analyzed because it is not directly addressed by the theory. Quantum MC simulations[18,19] provide quite good results in a rather large temperature region, but up to now they are only available for $S=1/2$.

As far as the different regimes of the 2DNLσM are concerned, the RCR is the most interesting (being the one linked with the real $S\geqslant 1/2$ compounds), but the QCR has also attracted much interest in recent years. CHN found that any 2DQNLσM with an ordered ground state crosses over from the RCR to the QCR at sufficiently high temperature. This statement cannot be trivially extended to the 2DQHAF, as we know that the relation between the two models only holds for low temperature. Nevertheless, the lower the spin, the lower the temperature at which such a crossover should occur, so that for sufficiently small S at least some signs of an intervening QCR-like regime could be detected.[21] As the correlation length of the 2DQNLσM in the QCR is $\xi \propto \alpha(T) = c/T$, such a sign could be, for instance, a temperature dependence of the measured ξ which becomes less pronounced as T increases. No such experimental evidence exists for pure compounds, but some doped materials show a similar behavior;[22] it has been argued that, by thinking of the doping as causing an effective increase of the quantum coupling, these experimental data could tell us that the doped magnet is undergoing a transition of the same nature of that between the renormalized classical and the QCR of the 2DQNLσM. This reasoning is still controversial and we will come back to this point at the end of Sec. V.

III. THE EFFECTIVE HAMILTONIAN

The effective Hamiltonian approach has been successfully applied in the last decade in the study of many different physical problems (for an extensive review see Ref. 23); the method is based on the path-integral formalism and allows us to express the quantum statistical average of physical observables in the form of classical-like phase-space integrals. Other methods in quantum statistical mechanics formally lead to this same form (see, e.g., Ref. 24), but they differ from each other because of the different approximations used to determine the effective phase-space density.

In the effective Hamiltonian method developed for a flat phase space, such approximation is the pure-quantum self-consistent harmonic approximation, whose name, though long, is at least self-explanatory. The PQSCHA does in fact separate the classical from the pure-quantum contribution to the thermodynamics of the system, and then approximates only the latter at a self-consistent harmonic level. This means that the classical physics is exactly described at any temperature, and so are the purely quantum linear effects, as the self-consistent harmonic approximation (SCHA) only affects the pure-quantum nonlinear contribution. In other words, we do not renounce the exact description of the classical behavior in its full nonlinearity just because we cannot deal with the nonlinear quantum corrections to it; we rather approximate only the latter. This result is specially valuable in the study of magnetic systems because their behavior is very often characterized by long-wavelength excitations (such as solitons, vortices, or Goldstone modes), whose character is indeed essentially classical.

The procedure leading to the effective Hamiltonian in the magnetic case[25] can be briefly summarized as follows. First of all, the spin Hamiltonian must be written in a bosonic form through a properly chosen spin-boson transformation. Secondly, the Weyl symbol[26] of the resulting bosonic Hamiltonian has to be determined and the quantum renormalizations[11] made explicit. Finally, the resulting effective Hamiltonian must be put into the form of a classical spin Hamiltonian (by the inverse of the classical counterpart of the spin-boson transformation used in the first step). The specific case of the 2DQHAF is described in Appendix B, where the detailed derivation of the effective spin Hamiltonian, that was just sketched in Ref. 6, is reported.

In choosing the spin-boson transformation for the isotropic Hamiltonian Eq. (1), we exclude the Villain transformation which is designed for models with easy-plane anisotropy. Furthermore, neither the Holstein-Primakoff[27] (HP) nor the Dyson-Maleev[28] (DM) transformation apparently gives an alternative, as they both break the symmetry of the problem. However, the broken symmetry of the (assumed ordered) ground state of the 2DQHAF is restored at finite temperature by long-wavelength excitations whose effect, as mentioned above, is almost entirely taken into account already at the classical level. As a consequence, it is almost entirely taken into account also by the PQSCHA, no matter what spin-boson transformation is used to evaluate the quantum renormalizations, as far as the bosonic effective Hamiltonian is eventually put into the form of a classical spin Hamiltonian. This means that by using the DM or HP transformation in the PQSCHA framework, we break the $O(3)$ symmetry, but only as far as the pure-quantum fluctuations are concerned, so that all the essential features due to the symmetry of the Hamiltonian are actually kept and the use of such transformations is consequently justified. As for the

choice between HP and DM, we employed the latter in Ref. 6; in Appendix A we show them to be equivalent in this context.

An important point is the ordering problem. Whenever a theory prescribes a function or functional to be associated with a quantum operator, it should also specify the ordering rule to be used for that purpose, to avoid an unnecessary uncertainty to enter the theory. When dealing with spin systems, such uncertainty often manifests itself in the ambiguous definition of the spin length, leading to an arbitrary choice between $S, \sqrt{S(S+1)}$, or others. The PQSCHA gives an unambiguous response to this point, by asking for the Weyl symbol of the quantum operator to enter the formulae for its own renormalization and, as we will see later, it makes the *effective spin length*

$$\widetilde{S}=S+\frac{1}{2} \tag{4}$$

naturally appear[6] (see Appendix A). Consistently with its being the spin length in this formalism, $\widetilde{S}$ sets the energy scale through the combination $J\widetilde{S}^2$. We therefore define the *reduced temperature* as

$$t\equiv\frac{T}{J\widetilde{S}^2}. \tag{5}$$

The final result for the effective spin Hamiltonian is

$$\frac{\mathcal{H}_{\rm eff}}{J\widetilde{S}^2}=-\frac{\theta^4}{2}\sum_{\mathbf{i},\mathbf{d}}\ \mathbf{s_i}\cdot\mathbf{s_{i+d}}+N\mathcal{G}(t), \tag{6}$$

$$\mathcal{G}(t)=\frac{t}{N}\sum_{\mathbf{k}}\ \ln\frac{\sinh f_k}{\theta^2 f_k}-2\kappa^2\mathcal{D}, \tag{7}$$

with the temperature and spin-dependent parameters

$$\theta^2=1-\frac{\mathcal{D}}{2}, \tag{8}$$

$$\mathcal{D}=\frac{1}{\widetilde{S}N}\sum_{\mathbf{k}}\ (1-\gamma_{\mathbf{k}}^2)^{1/2}\left(\coth f_{\mathbf{k}}-\frac{1}{f_{\mathbf{k}}}\right); \tag{9}$$

$$f_{\mathbf{k}}=\frac{\omega_{\mathbf{k}}}{2\widetilde{S}t}; \tag{10}$$

moreover, $\gamma_{\mathbf{k}}=(\cos k_1+\cos k_2)/2$, N is the number of sites of the lattice, and $\mathbf{k}\equiv(k_1,k_2)$ is the wave vector in the first Brillouin zone. $\mathcal{D}$ is the *pure-quantum* renormalization coefficient, which takes the main contribution from the high-frequency part (short-wavelength) of the spin-wave spectrum, because of the appearance of the Langevin function.

As for the frequencies $\omega_{\mathbf{k}}$, note that in the PQSCHA context they just appear in the evaluation of the pure-quantum renormalizations. In the general PQSCHA they depend upon the phase-space coordinate, but such dependence, when the system has many degrees of freedom, would make the evaluation of the phase-space integrals with the effective Hamiltonian a task as time demanding as a quantum MC simulation. Therefore, in deriving the above formulas, we have actually introduced a low-coupling approximation (LCA) to make the PQSCHA frequencies configuration independent (see Appendix B). On the other hand, since the effective Hamiltonian is affected by an approximate evaluation of the renormalized frequencies just at a secondary level, the approximation is worthy and assures the final results to depend only weakly on the specific LCA used.

There are in fact several ways of defining a possible LCA in this context. In Ref. 11, the fundamental phase-space-dependent parameters appearing in the theory (in terms of which the frequency are defined), say $A(\boldsymbol{p},\boldsymbol{q})$, were approximated in the simplest way as $A(\boldsymbol{p},\boldsymbol{q})\simeq A\equiv A(\boldsymbol{p}_0,\boldsymbol{q}_0)$; however, in the specific case of the 2DQHAF the minimum energy configuration becomes unstable as soon as the temperature is switched on, so that a more refined LCA is in fact necessary for a proper description of the low-temperature regime. In Ref. 11 we suggested for this case that $A(\boldsymbol{p},\boldsymbol{q})$ could be better approximated with its self-consistent average defined by the effective Hamiltonian, i.e.,

$$A(\boldsymbol{p},\boldsymbol{q})\simeq\frac{1}{\mathcal{Z}}\int d\boldsymbol{p}d\boldsymbol{q}\ A(\boldsymbol{p},\boldsymbol{q})e^{-\beta\mathcal{H}_{\rm eff}}\equiv\langle A(\boldsymbol{p},\boldsymbol{q})\rangle_{\rm eff}, \tag{11}$$

where $\mathcal{Z}$ is the partition function relative to $\mathcal{H}_{\rm eff}$. However, if an analytical expression for such averages is not available, this approximation does not actually lighten the burden of the numerical work. The best one can do analytically is to evaluate them in the framework of the classical SCHA. In Appendix B we show that this leads to two coupled equations that give us all the ingredients we need to actually use the effective Hamiltonian,

$$\omega_{\mathbf{k}}=4\kappa^2(1-\gamma_{\mathbf{k}}^2)^{1/2};$$

$$\kappa^2=1-\frac{1}{2}(\mathcal{D}+\mathcal{D}_{\rm cl})=\theta^2-\frac{\mathcal{D}_{\rm cl}}{2}, \tag{12}$$

where $\mathcal{D}_{\rm cl}=t/2\kappa^2$ represents the contribution to the frequency renormalization due to the classical part of the fluctuations; at variance with the pure-quantum coefficient $\mathcal{D}$, which is a decreasing function of temperature, $\mathcal{D}_{\rm cl}$ rises with t. As for the solution of the above equations, $\kappa^2(t)$ is real and positive for $t\leqslant\theta^4$, but becomes unphysically complex for $t>\theta^4$. From the explicit solution

$$\kappa^2=\frac{1}{2}[\,\theta^2+(\,\theta^4-t)^{1/2}] \tag{13}$$

one sees the instability to be originated just by the classical contribution to κ^2. This instability is typical of the SCHA and it is now shared by the PQSCHA because of the particular type of LCA chosen in order to optimize the low-temperature results. A closer look to Eqs. (12) shows that what causes the instability is the contribution to the frequency renormalization due to spin waves with long wavelength. On the other hand, linear excitations with $\lambda\gtrsim 2\xi$ are in fact unphysical as they do not exist in a system with no LRO; in their stead the system develops nonlinear excitations which are fundamental in determining the thermodynamics of the system, but whose contribution to the frequency renormalization is seen to be negligible by the same arguments showing them to be responsible for the vanishing of the magnetization.

Although the instability only affects the evaluation of the renormalized frequencies, we want to devise a reasonable way to treat it, in order to optimize the description of the temperature region where the above mentioned nonlinear excitations become relevant in the thermodynamics of the system, which is in fact the same region where the instability occurs. The unphysical contribution in Eqs. (12) is then pulled up by inserting a cutoff $|\mathbf{k}| \gtrsim \pi/\xi$, over the AFM Brillouin zone, in the evaluation of $\mathcal{D}_{\rm cl}$. Such a cutoff is obviously t dependent, being $\xi = \xi(t)$, and it is relevant in the temperature region where quantum nonlinear excitations are most important in the system. As we will see in Sec. V, such region seems to coincide with that where other authors devised anomalous behaviors, ascribed to the occurrence of quantum criticality in the theoretical works,[21] or to doping effects in the experimental ones.[29]

Coming back to the effective Hamiltonian (6), we see the quantum effects to cause (i) the appearance of the spin length $\tilde{S}$, (ii) the renormalization of the exchange integral J by the factor $\theta^4(t) < 1$, (iii) the introduction of a uniform term $\mathcal{G}(t)$.

As far as $\mathcal{G}(t)$ is concerned, although it does not play any role in calculating thermal averages, it contains the essential logarithmic term that transforms the spin-wave contribution to the free energy from classical to quantum.[11] At $t=0$, $\mathcal{G}(0)=0$ and the zero-temperature energy per site is $-2\theta^4(0)$, higher than the classical value -2, because of the zero-point quantum fluctuations. We have already commented on the appearance of $\tilde{S}$ as a consequence of a precise ordering prescription; we just add here that this is a genuine quantum effect, being the noncommutativity of quantum operators the only reason for an ordering rule to be necessary.

Let us now examine the exchange-integral renormalization embodied in the factor θ^4; the parameter θ^2 depends on both S and t, it is well defined as far as a physical solution for κ^2 is available; it attains its minimum value for $t=0$, where $\theta^2 = \kappa^2$ coincides with the one-loop correction to the spin-wave velocity. For increasing S or t, θ^2 increases, going asymptotically to 1 in the classical ($S \to \infty$) or high-temperature ($t \to \infty$) limit. The instability value $\theta^2 = 0$ is not reached for physical values of the spin, being $\theta^2 > 1 - (2\tilde{S})^{-1} > 0$ for $S > 0$.

The essential information we get from Eq. (6) is that the 2DQHAF at an actual temperature t behaves as its classical counterpart at an effective temperature

$$t_{\rm eff} = \frac{t}{\theta^4(t)}, \tag{14}$$

or, in other terms, that the energy scale is renormalized by a temperature dependent factor $\theta^4(t)$. In Figs. 1 and 2 we show θ^4 and $t_{\rm eff}$ as functions of t, for different spins, including some $S < 1/2$ unphysical values (dotted lines). As S decreases the difference between t and $t_{\rm eff}$ becomes more and more pronounced, because of θ^2 getting smaller, indicating larger quantum fluctuations in the system.

Our theory is quantitatively meaningful just as far as the renormalization coefficient $\mathcal{D}$ is small enough to justify the self-consistent harmonic treatment of the pure-quantum effects; although this is not obviously the case for the $S < 1/2$ low-temperature regime, the dotted lines at least qualitatively suggest that no critical behavior occurs, no matter how small the spin value. What we rather see is that the sharp dependence of $t_{\rm eff}$ upon t brings to lower temperatures those features which are indeed typical of the highly disordered, high-temperature regime of the classical model. In Sec. V C we will come back to this point, in relation with the effects of magnetic doping, and we just recall here that any reasoning about models with $S < 1/2$ should just be considered as speculative when dealing with real magnets.

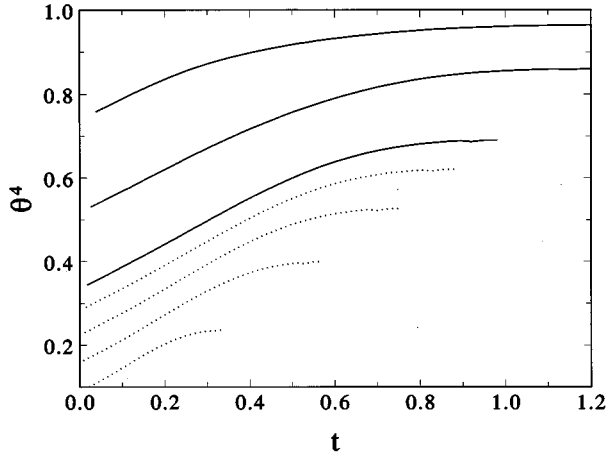

FIG. 1. Renormalization parameter θ^4 vs t, for (from the top curve) $S = 5/2$, 1, 1/2 (solid lines), and $S = 0.4$, 0.3, 0.2, 0.1 (dotted lines).

IV. THERMODYNAMIC PROPERTIES

Once the effective Hamiltonian has been determined, the thermodynamic properties can be derived from the partition function $\mathcal{Z} = \int d\boldsymbol{p} d\boldsymbol{q} \exp(-\beta \mathcal{H}_{\rm eff})$; more general statistical averages are given by

$$\langle \hat{\mathcal{O}} \rangle = \frac{1}{\mathcal{Z}} \int d^N \boldsymbol{s} \tilde{\mathcal{O}} e^{-\beta \mathcal{H}_{\rm eff}} \equiv \langle \tilde{\mathcal{O}} \rangle_{\rm eff}, \tag{15}$$

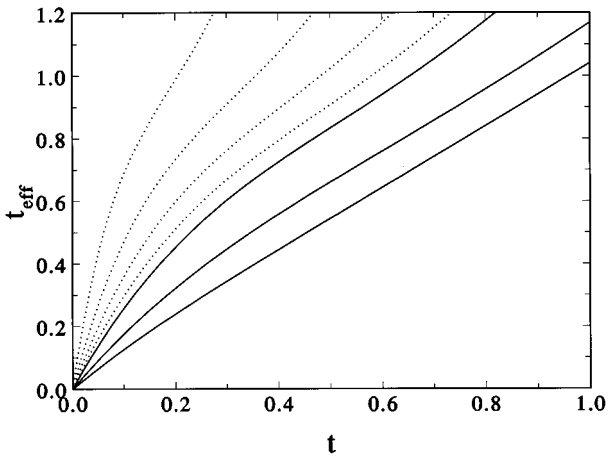

FIG. 2. Effective classical temperature $t_{\rm eff} = t/\theta^4(t)$ vs t, for (from the bottom curve) $S = 5/2$, 1, 1/2 (solid lines) and $S = 0.4$, 0.3, 0.2, 0.1 (dotted lines).

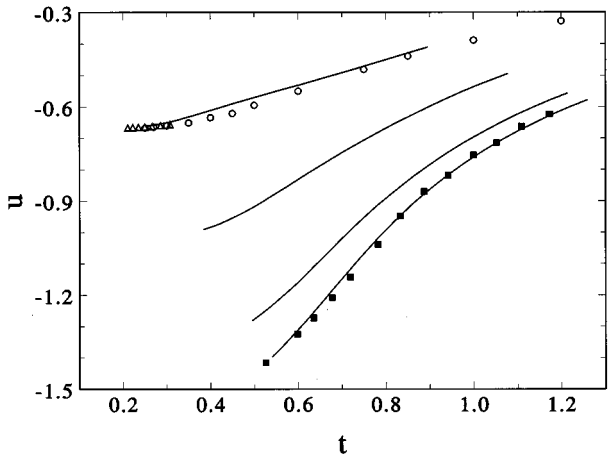

FIG. 3. Energy per spin $u=\langle\hat{\mathcal{H}}\rangle/(NJ\widetilde{S}^2)$ vs t, for (from the bottom curve) $S=\infty$, 5/2, 1, and 1/2; the symbols are quantum MC data for $S=1/2$ [circles (Ref. 18) and triangles (Ref. 19)] and previous classical MC data (Ref. 16) (squares).

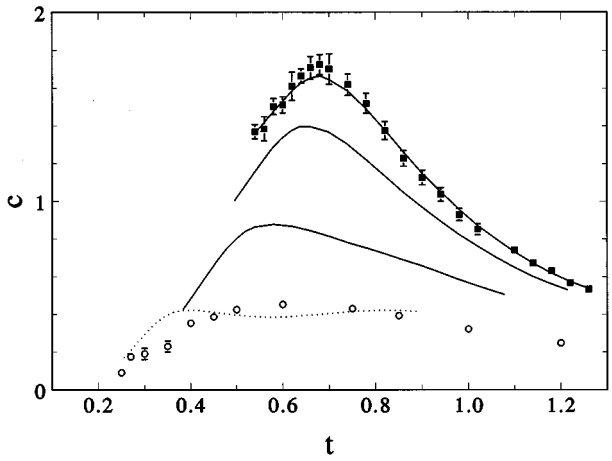

FIG. 4. Specific heat per spin $c\equiv\partial u/\partial t$ vs t, for (from the top curve) $S=\infty$, 5/2, 1 and 1/2; circles as in Fig. 3; squares are our MC results. For the (dotted) $S=1/2$ curve see comments in the text.

where $\widetilde{\mathcal{O}}\equiv\widetilde{\mathcal{O}}(\{\mathbf{s_i}\})$ is obtained by the quantum operator $\hat{O}$ following the same procedure used to determine the configurational part of $\mathcal{H}_{\rm eff}$ (see Appendix B); by $\langle\cdots\rangle_{\rm eff}$ we hereafter mean the classical thermal average with the effective Hamiltonian, which equals the classical average at the effective temperature $t_{\rm eff}$.

In order to evaluate the classical 2D phase-space integrals appearing in $\langle\cdots\rangle_{\rm eff}$ according to Eq. (15), a standard classical MC simulation is perfectly suitable; being the existent classical MC data[16,17] incomplete as far as the correlation functions are concerned, we have performed our own simulations (following the same procedure described in Ref. 30, with slight modifications of the overrelaxed moves made to account for the fully isotropic exchange) on a 256×256 square lattice, for $0.54\leqslant t\leqslant1.42$. The dimension of the lattice ensures the data to be free from saturation effects, according to the $L\gtrsim6\xi$ criterion, for all temperatures but the first two (0.54 and 0.56).

A. Internal energy and specific heat

According to Eq. (15), the internal energy per spin $u\equiv\langle\hat{\mathcal{H}}\rangle/(NJ\widetilde{S}^2)$ is

$$u(t)=\theta^4(t)u_{\rm cl}(t_{\rm eff}), \tag{16}$$

where $u_{\rm cl}$ is the classical energy; from the results shown in Fig. 3 we see the quantum renormalizations to increase the energy and flatten the curve $u(t)$ at all temperatures and more markedly for smaller spin. Quantum fluctuations are responsible for both effects, as they introduce additional and almost temperature-independent disorder, thus making the system more unstable, i.e., with many different configurations thermodynamically relevant, already at low temperatures.

Consistently with this picture, Fig. 4 shows the peak of the specific heat moving towards lower temperatures and decreasing in height, as S decreases. Our data for the specific heat at finite spin are obtained by numerical derivation of $u(t)$, as given by Eq. (16); because of the temperature dependence of the cutoff involved in the LCA (as described in Sec. III), they are affected by consistent numerical uncertainty and should not be considered but qualitatively for $S=1/2$ where such dependence is more pronounced.

B. Correlation functions

For the correlation functions $G(\mathbf{r})\equiv\langle\hat{\mathbf{S}}_\mathbf{i}\cdot\hat{\mathbf{S}}_{\mathbf{i}+\mathbf{r}}\rangle$, with $\mathbf{r}\equiv(r_1,r_2)$ any vector on the square lattice, we find (see Appendix B)

$$G(\mathbf{r})=\widetilde{S}^2\theta_\mathbf{r}^4\langle\mathbf{s_i}\cdot\mathbf{s}_{\mathbf{i}+\mathbf{r}}\rangle_{\rm eff}, \tag{17}$$

where $\theta_\mathbf{r}^4=1-\frac{1}{2}\mathcal{D}_\mathbf{r}$ and the renormalization parameter $\mathcal{D}_\mathbf{r}$ reads

$$\mathcal{D}_\mathbf{r}=\frac{1}{\widetilde{S}N}\sum_\mathbf{k}\left(\frac{1+\gamma_\mathbf{k}}{1-\gamma_\mathbf{k}}\right)^{1/2}\left(\coth f_\mathbf{k}-\frac{1}{f_\mathbf{k}}\right)(1-\cos\mathbf{k}\cdot\mathbf{r}); \tag{18}$$

note that for nearest neighbors, $\mathbf{r}=\mathbf{d}$, we have $\mathcal{D}_\mathbf{d}\equiv\mathcal{D}$.

Equation (17) shows that the quantum correlation functions can be obtained by multiplying the classical ones at the effective temperature $t_{\rm eff}$ by the temperature and spin-dependent renormalization factor $\theta_\mathbf{r}^4\widetilde{S}^2$. The overall effect is that of a strong reduction of the spin correlations, as it is clear from Fig. 5, where $G^*(r)\equiv|G(|\mathbf{r}|)|/\widetilde{S}^2$ is shown for $\mathbf{r}=(r,0)$, at a fixed temperature and for different values of the spin.

In order to exploit some available quantum MC data for $S=1/2$, we have performed four classical MC simulations with the effective Hamiltonian, at the temperatures corresponding, via Eq. (14), to those at which quantum MC simulations have been performed by Makivić and Ding.[18] As seen in Fig. 6, the agreement we find is very good, and gives us confidence to proceed towards the evaluation of the susceptibility and of the correlation length, both indeed deriving from the correlation functions.

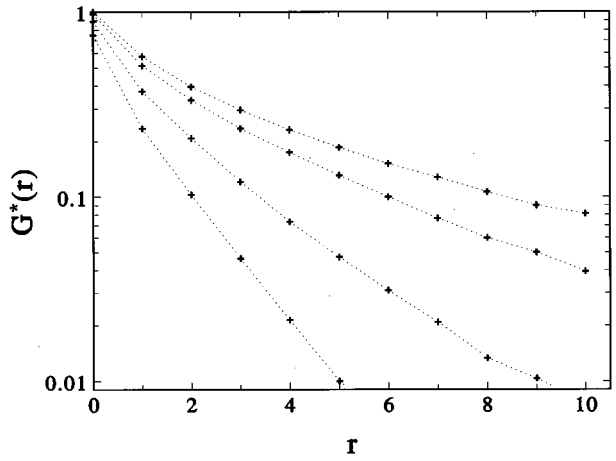

FIG. 5. Absolute value of the spin correlation function $G^*(r)=|G(r,0)|/\tilde{S}^2$ vs r, at $t=0.7$ and for (from the top curve) $S=\infty$, 5/2, 1, and 1/2; the dotted lines are just guides for the eye.

V. FACING THE EXPERIMENTAL DATA

In this last section we compare our results with the available experimental data and show that, at variance with what seems to emerge from the analysis based on the QNLσM approach, there is no substantial difference between the agreement we find for systems with $S=1/2$, and those with $S=1$.

We consider two fundamental physical observables, the staggered susceptibility χ and the correlation length ξ, and we underline once more that our results do not contain free parameters and need nothing but the values of J and S to be compared with the experimental data. In the case of the staggered susceptibility, the latter come in arbitrary units so that a multiplicative factor must be determined by the standard least-squares procedure. We also remind that our results for $S=1/2$ and low temperatures ($t\lesssim 0.35$) are obtained in a region where the PQSCHA, given the relatively large value of the renormalization coefficient $\mathcal{D}$, touches its limit of validity.[31]

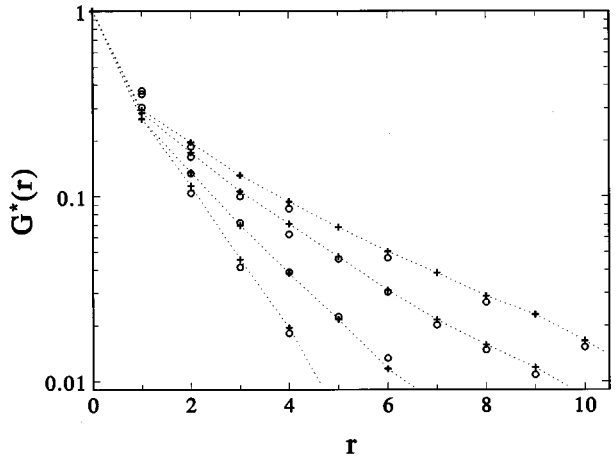

FIG. 6. Absolute value of the spin correlation function $G^*(r)=|G(r,0)|/\tilde{S}^2$ vs r, at $S=1/2$ and for (from the top curve) $t=0.45$, 0.50, 0.60, 0.75; also reported are quantum MC data (Ref. 18) (circles). The dotted lines are just guides for the eye.

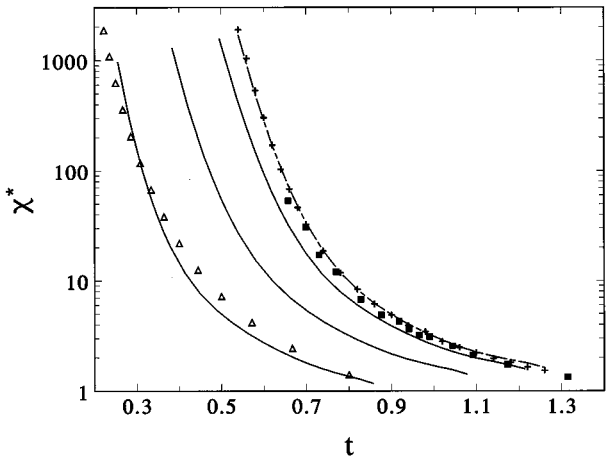

FIG. 7. Staggered susceptibility $\chi^*=\chi/\tilde{S}^2$ vs t, for (from the rightmost curve) $S=\infty$, 5/2, 1, and 1/2; the crosses (our simulations, see text) and the squares (Ref. 16) are classical MC data, the triangles are quantum MC data (Ref. 19) for $S=1/2$.

A. The staggered susceptibility

The staggered susceptibility for the 2DQHAF is defined as

$$\chi=\frac{1}{3}\sum_{\mathbf{r}}(-)^{r_1+r_2}G(\mathbf{r}) \tag{19}$$

and by the PQSCHA result Eq. (17) we find

$$\chi=\frac{1}{3}\left[S(S+1)+\tilde{S}^2\sum_{\mathbf{r}\neq 0}(-)^{r_1+r_2}\theta_{\mathbf{r}}^4\langle \mathbf{s_i}\cdot\mathbf{s_{i+r}}\rangle_{\text{eff}}\right]. \tag{20}$$

By using our classical MC data for $\langle \mathbf{s_i}\cdot\mathbf{s_{i+r}}\rangle_{\text{eff}}$ we then obtain the quantum results for all values of S, as the spin- and temperature-dependent renormalization factor $\theta_{\mathbf{r}}^4$ can be easily evaluated for any value of $\mathbf{r}$.

In Fig. 7 we show $\chi^*\equiv\chi/\tilde{S}^2$ as a function of temperature for different spin values. For $S=\infty$ we have reported our MC data, as obtained from both the general definition (20) (curve) and the classical expression $\chi^*=\langle|\Sigma_{\mathbf{i}}\mathbf{s_i}|^2\rangle/3N$ (crosses); also reported are classical MC data from Ref. 16, as well as quantum MC data recently obtained by Kim *et al.*[19] for $S=1/2$. Figure 8 shows our results for $S=1/2$ together with experimental data[12] for the real compound $Sr_2CuO_2Cl_2$; the quantum MC results by Makivić and Ding are also shown. The case $S=1$ is considered in Fig. 9, where the experimental data[13,12] for the compounds La_2NiO_4 and K_2NiF_4 are reported. The agreement between our theoretical curves and the experimental data is substantially equivalent in both the $S=1/2$ and $S=1$ case, strongly suggesting that the difficulties encountered by a QNLσM-based analysis to draw a unique picture for different spin values, derive from the inadequacy of the theory, rather than from an actual difference in the thermodynamics of the different compounds.

B. Correlation length

The correlation length is defined by the asymptotic behavior for $r\equiv|\mathbf{r}|\to\infty$ of the correlation function, $|G(\mathbf{r})|\sim e^{-r/\xi}$. From the PQSCHA result, Eq. (17), since for large r

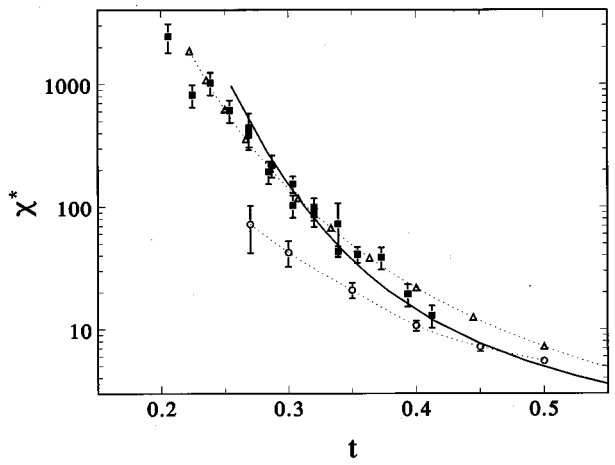

FIG. 8. Staggered susceptibility $\chi^*=\chi/\tilde{S}^2$ vs t, for $S=1/2$. Circles (Ref. 18) and triangles (Ref. 19) are quantum MC data (the dotted lines are just guides for the eye); the squares are neutron scattering data (Ref. 12) for $Sr_2CuO_2Cl_2$.

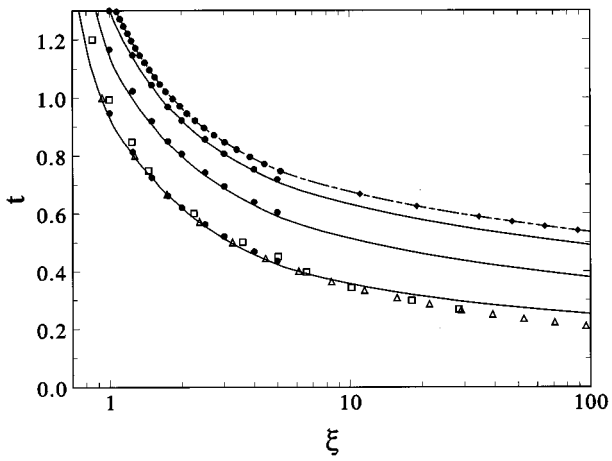

FIG. 10. Curves $t(\xi)$ as explained in text, for (from the top curve) $S=\infty$, $S=5/2$, 1, and $1/2$, the triangles (Ref. 19) and the squares (Ref. 18) are quantum MC data for $S=1/2$, the circles are HTE results (Ref. 10), and the diamonds are classical MC data (Ref. 17).

$\theta_{\mathbf{r}}^4\to$const, we get $\langle \mathbf{s_i}\cdot\mathbf{s_{i+r}}\rangle_{\rm eff}\sim e^{-r/\xi}$, which means, comparing the definition (15) and using Eq. (14),

$$\xi(t)=\xi_{\rm cl}(t_{\rm eff}), \tag{21}$$

i.e., the correlation length ξ of the quantum model at a certain temperature t equals the classical one $\xi_{\rm cl}$ at the effective temperature $t_{\rm eff}>t$. It is easy to see that the relation empirically extracted by Elstner *et al.*[10] from their HTE results (i.e., $\xi(S,T)\approx\xi_{\rm cl}[T/JS(S+1)]$ for $S>1$ and $T\gtrsim JS$) is nothing but the high-T and high-S limit of Eq. (21). Furthermore, Eq. (21) represents the correct expression of the link between the classical and the quantum discrete magnetic model, to be compared with the one devised by CHN for the QNLσM in the renormalized classical regime, leading from the classical result by Brézin and Zinn-Justin[32] to Eq. (2).

Equation (21) allows us to obtain the quantum correlation length from the classical one by a simple temperature scaling. In other terms, we see that each value ξ corresponds to a temperature $t(\xi,S)$ which is different for different spin values. This point of view is taken in Fig. 10, where we report our results for $t(\xi,S)$, together with MC and HTE data. In the $S=1/2$ case, we find that $t(\xi,1/2)/t(\xi,\infty)=\theta^4\gtrsim 0.5$ for $\xi\gtrsim 10$; as already pointed out at the end of Sec. III, such a small value of θ^4 makes the PQSCHA no more quantitatively reliable. Nevertheless, the figure shows that the accuracy of our results for $t(\xi,S)$ at $S=1/2$ and $\xi\simeq 100$, as from the comparison with the quantum MC data, is still better than 20%, which makes them qualitatively meaningful even in the extreme quantum region.[31] However, the inaccuracy in the ''renormalized'' temperature gives larger inaccuracy in the inverse function, $\xi(t)$, due to its exponential behavior.

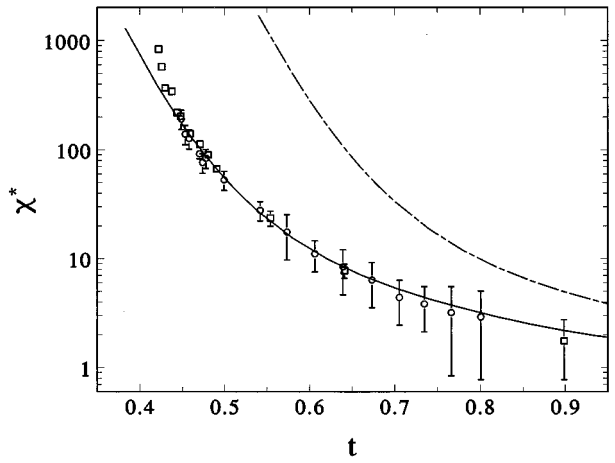

FIG. 9. Staggered susceptibility $\chi^*=\chi/\tilde{S}^2$ vs t, for $S=1$. Circles and squares are neutron scattering data for La_2NiO_4 (Ref. 13) and K_2NiF_4 (Ref. 12), respectively. The classical result (dash-dotted line) is also reported.

The experimental data for $S=1/2$ and $S=1$ are compared with our theory in Fig. 11; at variance with what happens by using the QNLσM approach, the agreement does not get worse in the $S=1$ case. For each spin we have also reported the curves (dashed lines) obtained by using the standard LCA (high-t curves) as well as the more accurate one described in Sec. III (low-t curves) without cutoff and hence truncated at $t=\theta^4$. They are smoothly connected by the continuous curves, i.e., those obtained by using the cutoff. For each spin value, the temperature interval where the cutoff is relevant identifies the region where nonlinear excitations are present in the system, and hence suggests where a possible crossover towards the QCR could occur.

In order to better understand why the QNLσM theory fails in describing the 2DQHAF when used to interpret the available reference data for $S\gtrsim 1$, the function $y(t)=t\ln\xi$ is shown in Fig. 12 as a function of t. We remind the reader that the QNLσM approach gives $y_{\rm q}(t)=mt+n$ in the quantum case (with m and n constant in temperature but S dependent), being such expression based on the classical two-loop result $y_{\rm cl}(t)=t\ln(\mu t)+\nu$ (with μ and ν constants); first of all, one must check whether or not this classical result can be safely extended to the magnetic system.

Let us concentrate on the $S=\infty$ (classical) MC data re-

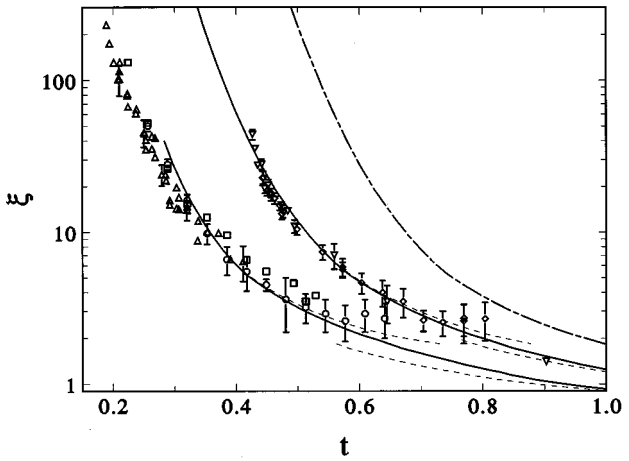

FIG. 11. Correlation length ξ vs t, for $S=1/2$ (leftmost) and $S=1$. The symbols are experimental data; for $S=1/2$: ^{63}Cu NQR data (Ref. 14) (circles) and neutron scattering data for La_2CuO_4 [squares (Ref. 15)] and for $Sr_2CuO_2Cl_2$ [up-triangles (Ref. 12)]; for $S=1$: neutron scattering data for La_2NiO_4 [down-triangles (Ref. 13)] and for K_2NiF_4 [diamonds (Ref. 12)]. The classical result (dash-dotted line) is also reported; the dashed lines are the low-t and high-t results of the PQSCHA (see text).

ported in Fig. 12 (rightmost curve): The complete curve cannot be fitted with a function of the form y_{cl} and such a fit is solely possible if one restricts himself to a limited temperature range, as in the intermediate-temperature region there is a clear change in the slope. On the other hand, this should not surprise, as $t\ln\xi = t\ln(\mu t)+\nu$ is a two-loop result and it is hence bound to be correct only at lowest temperatures. We now expect this problem to propagate to the quantum case, which is based on the classical result.

Let us then look at the $S=5/2$ and $S=1$ curves: according to the QNLσM these should be straight lines, but they are

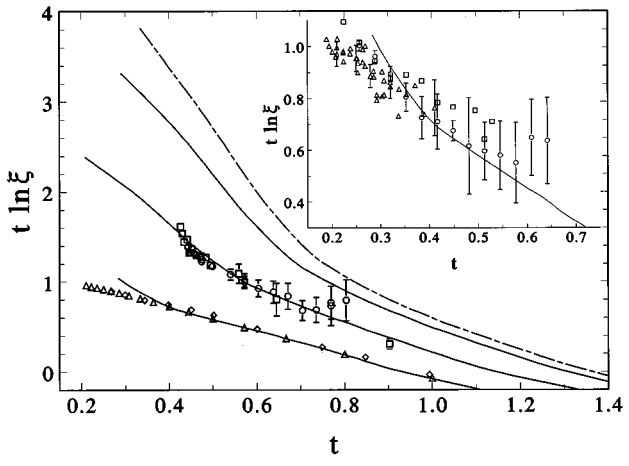

FIG. 12. The function $y(t)=t\ln\xi$ vs t, for (from the rightmost curve) $S=\infty$, 5/2, 1, and 1/2; the triangles (Ref. 19) and the diamonds (Ref. 18) are quantum MC data for $S=1/2$. Also reported are neutron scattering data for La_2NiO_4 [circles (Ref. 13)] and for K_2NiF_4 [squares (Ref. 12)]. The inset reports, together with our result for $S=1/2$ (line), ^{63}Cu NQR data [circles (Ref. 14)] and neutron scattering data for La_2CuO_4 [squares (Ref. 15)] and for $Sr_2CuO_2Cl_2$ [triangles (Ref. 12)].

not; actually one can easily see a change in the slope at intermediate temperature, followed by a curvature inversion at lower t. As in the classical case, hence, good fits with the function y_q can be obtained either in the low- or (misleadingly) in the high-temperature region, but not on the whole temperature range. To fit the experimental data for $S=1$ with a straight line is seemingly impossible, as pointed out by several authors[10,12,13] in the past few years.

Finally, if we look at the $S=1/2$ case it becomes clear why the QNLσM approach gave such a good agreement when first used to fit the experimental data. The change in both the slope and the curvature of $t\ln\xi$ is less pronounced and possibly occurs at lower temperatures, the lower the spin: in the $S=1/2$ case, we find difficult to say whether these features are still present or not, but, if yes, they occur in a temperature region where the extremely high value of ξ ($\approx 10^4$) makes both the experimental and the simulation data more difficult to be obtained. The experimental data, as well as our results, do actually suggest a change in the slope; on the other hand quantum MC data by Kim *et al.*,[19] do not give evidence of such change.

As for the very-low temperature data by Suh *et al.*,[33] it is to be noticed that the authors explained the change in the slope of their curve in terms of a crossover from an isotropic towards an easy-plane (Kosterlitz-Thouless-like) behavior. We cannot question their interpretation, but we underline that their conclusion is based on the assumption that the $t\ln\xi$ curve for the 2DQHAF is a straight line, which is, as we are seeing, at least questionable.

C. Magnetic doping and quantum criticality

We have already pointed out that at intermediate temperatures there is an interval, whose width is larger the smaller the spin, where quantum nonlinear effects (due to higher order terms in the coupling) are significant; such interval is identified, in our theory, by the temperature region where the cutoff is relevant, a region which is very easily recognizable in Fig. 11 ($0.45\lesssim t\lesssim 0.9$ for $S=1/2$ and $0.65\lesssim t\lesssim 1$ for $S=1$) and seems indeed to coincide with that where Chubukov and Sachdev[34] suggested the occurrence of the QCR in the QNLσM.

Experimental data for magnetically doped materials have been interpreted by several authors in terms of a possible crossover from the classical renormalized towards the QCR. Let us concentrate, in particular, on the data by Carretta *et al.*,[29] obtained by a scaling analysis of their ^{63}Cu nuclear quadrupole relaxation (NQR) data, for the correlation length of La_2CuO_4 doped with nonmagnetic impurities, i.e., for the compound $La_2Cu_{1-x}Zn_xO_4$. In Fig. 13 we report their data for $x=0.018$: it is evident that the doping causes a strong reduction of the spin correlation, as well as a clear flattening of ξ as a function of temperature. Such flattening does occur in the same intermediate temperature region where the QCR has been suggested to occur.

The authors have interpreted their data in terms of an effective reduction of the spin stiffness, consistently with our theory which shows similar effects to be caused by an effective reduction of the spin value. The curve in Fig. 13 is obtained by the PQSCHA with $S=0.35$, a value which has been empirically determined in order to optimize the agree-

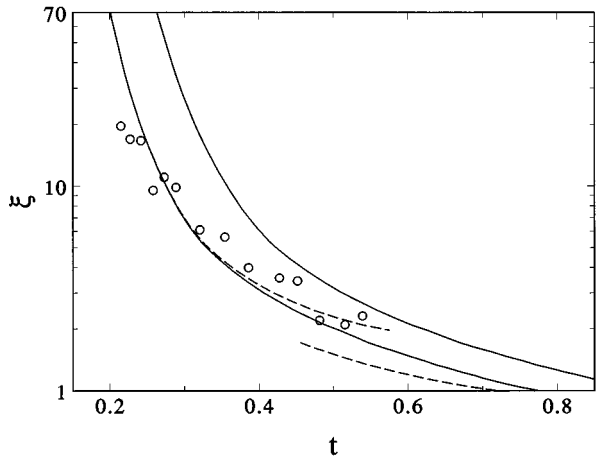

FIG. 13. Experimental data for the correlation length, for the magnetically doped compound $La_2Cu_{1-x}Zn_xO_4$, from Ref. 29. The leftmost lines refer to $S=0.35$, with the dashed lines as in Fig. 11; for comparison the $S=1/2$ curve is also reported (rightmost curve).

ment with the experimental data. Although the use of our approach for $S<1/2$ is not fully justified, these results do at least qualitatively suggest that for $S<1/2$ the magnetic model moves towards a regime where nonlinear effects become relevant in a wider temperature region (the one where ξ shows a clear plateau) and such behavior could be seen as a signature of the crossover towards a QCR.

VI. CONCLUSIONS

In this paper we have applied the pure-quantum self-consistent harmonic approximation[11] (PQSCHA) to the study of the thermodynamics of the two-dimensional Heisenberg antiferromagnet on the square lattice. The PQSCHA allowed us to reduce the evaluation of quantum averages to the calculation of classical-like phase-space integrals. Therefore, using classical MC simulations, we have been able to obtain results for several quantum thermodynamic quantities. What is remarkable is that these results are fully determined by the system's parameters, i.e., the spin value S and the ratio between the temperature and the exchange energy constant T/J.

The main effect is seen to be the temperature-dependent weakening of the effective classical exchange constant, so that an effective classical temperature naturally arises, Eq. (14); this leads to a very simple relation, Eq. (21), directly giving the quantum correlation length in terms of its classical counterpart. For other thermodynamic quantities, such as correlation functions and the staggered susceptibility, the expressions involve further pure-quantum renormalization factors that can be straightforwardly computed. Even pushing down the theory to the extreme quantum case, $S=1/2$, we find agreement both with quantum MC and experimental data, until the renormalization parameters of the theory become too large for $T/J \lesssim 0.35$ making the results of only qualitative value.

For higher spin, $S \geqslant 1$, the theory is reliable at any temperature, and it agrees indeed with the available experimental data, while quantum MC simulations have not yet been feasible. It would be interesting to compare also with the announced[10] experimental results for the $S=5/2$ square-lattice antiferromagnet Rb_2MnF_4, which are not yet available.

ACKNOWLEDGMENTS

We acknowledge hospitality at the ISIS Facility of the Rutherford Appleton Laboratory (U.K.), where part of this work and most of the related classical MC simulations were performed, and we thank S. W. Lovesey, head of the ISIS theory division. V.T. acknowledges fruitful exchanges of visits and discussions with F. Borsa and A. V. Chubukov. We thank A. Rigamonti and P. Carretta, for useful discussion and for providing us with experimental data, and J.-K. Kim, D. P. Landau, and M. Troyer for their useful comments and for supplying unpublished quantum MC data.

APPENDIX A: SPIN-BOSON TRANSFORMATION AND WEYL ORDERING

In this appendix we compare the Dyson-Maleev[28] (DM) and the Holstein-Primakoff[27] (HP) transformations as far as the ordering problem is concerned. The DM transformation for the spin operators $\hat{S}^{\pm} \equiv \hat{S}^x \pm i\hat{S}^y$ and $\hat{S}^z$, in terms of bosonic operators $(\hat{a}^\dagger, \hat{a})$ is

$$\hat{S}^+ = (2S)^{1/2}\hat{a},$$

$$\hat{S}^- = (2S)^{-1/2}\hat{a}^\dagger(2S - \hat{a}^\dagger\hat{a}),$$

$$\hat{S}^z = S - \hat{a}^\dagger\hat{a}. \tag{A1}$$

The transformation is canonical, as from $[\hat{a}, \hat{a}^\dagger] = 1$ the spin commutation relations follow, with $|\hat{\boldsymbol{S}}|^2 = S(S+1)$. Their Weyl symbols are found to be[6]

$$S^+ = (2S)^{1/2}a,$$

$$S^- = (2S)^{-1/2}(2\widetilde{S} - a^*a)a^*,$$

$$S^z = \widetilde{S} - a^*a. \tag{A2}$$

For the use of the DM transformation in the 2DQHAF context we refer to Ref. 6.

The HP transformation reads instead

$$\hat{S}^+ = (2S - \hat{a}^\dagger\hat{a})^{1/2}\hat{a},$$

$$\hat{S}^- = (\hat{S}^+)^\dagger,$$

$$\hat{S}^z = S - \hat{a}^\dagger\hat{a}, \tag{A3}$$

and can be rewritten in terms of phase-space operators $\hat{q} = (\hat{a}^\dagger + \hat{a})/(2\widetilde{S})^{1/2}$ and $\hat{p} = i(\hat{a}^\dagger - \hat{a})/(2\widetilde{S})^{1/2}$, where $\widetilde{S} = S + 1/2$ and with commutator $[\hat{q}, \hat{p}] = i/\widetilde{S}$, as

$$\hat{S}^+ = \widetilde{S}\left[1-\frac{1}{4}\left(\hat{q}^2+\hat{p}^2+\frac{1}{\widetilde{S}}\right)\right]^{1/2}(\hat{q}+i\hat{p}),$$

$$\hat{S}^- = (\hat{S}^+)^\dagger,$$

$$\hat{S}^z = \widetilde{S}\left(1-\frac{\hat{q}^2+\hat{p}^2}{2}\right). \tag{A4}$$

We have now to determine the Weyl symbols of these operators; indicating with A_W the Weyl symbol of the operator $\hat{A}$, the following product relation[26] holds:

$$(AB)_W = A_W \exp\left[-\frac{i}{2\widetilde{S}}(\overleftarrow{\partial}_p\overrightarrow{\partial}_q-\overleftarrow{\partial}_q\overrightarrow{\partial}_p)\right]B_W. \tag{A5}$$

Let us start with the operator $\hat{S}^+$, which has indeed the form of the product of two Weyl-ordered operators, $\hat{S}^+ = \widetilde{S}\hat{A}\hat{B}$, with

$$A_W = \left[1-\frac{1}{4}\left(q^2+p^2+\frac{1}{\widetilde{S}}\right)\right]^{1/2} \equiv \sum_n c_n (q^2+p^2)^n \tag{A6}$$

and $B_W = q+ip$, where the coefficients c_n arise from the expansion of the square root. By using Eq. (A5) we then find

$$\begin{aligned}(AB)_W &= \sum_n c_n (q^2+p^2)^n e^{-i(\overleftarrow{\partial}_p\overrightarrow{\partial}_q-\overleftarrow{\partial}_q\overrightarrow{\partial}_p)/2\widetilde{S}}(q+ip)\\ &= \sum_n c_n (q^2+p^2)^n\left[q+ip-\frac{1}{2\widetilde{S}}(\overleftarrow{\partial}_q+i\overleftarrow{\partial}_p)\right]\\ &= \sum_n c_n\left[(q^2+p^2)^n-\frac{n}{\widetilde{S}}(q^2+p^2)^{n-1}\right](q+ip)\\ &\approx \sum_n c_n\left(q^2+p^2-\frac{1}{\widetilde{S}}\right)^n(q+ip)\\ &= \left[1-\frac{1}{4}(q^2+p^2)\right]^{1/2}(q+ip),\end{aligned} \tag{A7}$$

where terms up to the first order in $1/\widetilde{S}$ have been kept; hence, being $S^- = (S^+)^*$ and the operator $\hat{S}^z$ in Eq. (A4) already Weyl ordered, the Weyl symbols of the HP operators are

$$S^\pm = \widetilde{S}\left[1-\frac{1}{4}(q^2+p^2)\right]^{1/2}(q\pm ip),$$

$$S^z = \widetilde{S}\left(1-\frac{q^2+p^2}{2}\right). \tag{A8}$$

Note that the value $\widetilde{S} \equiv S+\frac{1}{2}$ appears as the natural spin length of the theory, being $|\boldsymbol{S}|^2 = (S^z)^2 + S^+S^- = \widetilde{S}^2$, both in the DM case (A2) and in the HP case (A8).

In the above derivation for the HP case we have neglected terms of the order $1/\widetilde{S}^2$ and higher: this approximation is necessary to obtain reasonably simple expressions of $S^\pm_W$. Although no such approximation seems to appear when using the DM transformation, this is in fact a wrong conclusion. Indeed, it is well known that, in order to apply the DM transformation, and properly take into account the kinematic interaction, one should use, rather than the simple transformed Hamiltonian $\hat{\mathcal{H}}_{\rm DM}$, the operator $\hat{P}\hat{\mathcal{H}}_{\rm DM}\hat{P}$ where $\hat{P}$ is the projector on the Hilbert subspace of the spin system. Such subspace is generated by the eigenstates of the operator $\hat{a}^\dagger\hat{a}$ with positive eigenvalues $n \leqslant 2S$, i.e., by the eigenstates of the operator $\hat{z}^2 \equiv (\hat{q}^2+\hat{p}^2)/2$ with $2\widetilde{S}$ equispaced positive eigenvalues $0 \leqslant z^2 \leqslant (2-1/2\widetilde{S})$. On the other hand, to determine the explicit form of the Weyl symbol for the operator $\hat{P}\hat{\mathcal{H}}_{\rm DM}\hat{P}$ is an impossible task, unless one only keeps terms up to the first order in $1/\widetilde{S}$; this means to approximate $\hat{P}$ with the identity operator, which is in fact what we have done in Sec. III. Both transformations can hence be used in the framework of the PQSCHA and do actually involve the same semiclassical approximation.

APPENDIX B: THE EFFECTIVE SPIN HAMILTONIAN

The general expression given by the PQSCHA for the LCA effective Hamiltonian is[11]

$$\mathcal{H}_{\rm eff} = e^{\Delta}\mathcal{H}(\boldsymbol{p},\boldsymbol{q}) - \sum_{\mathbf{k}} \alpha_{\mathbf{k}}\omega_{\mathbf{k}}^2 + \frac{1}{\beta}\sum_{\mathbf{k}} \ln\frac{\sinh f_{\mathbf{k}}}{f_{\mathbf{k}}}, \tag{B1}$$

where $\mathcal{H}(\boldsymbol{p},\boldsymbol{q})$ is the Weyl symbol of the original Hamiltonian $\hat{\mathcal{H}}$ and

$$\Delta = \frac{1}{2}\sum_{\mathbf{ij}} [D^{(pp)}_{\mathbf{ij}}\partial_{p_\mathbf{i}}\partial_{p_\mathbf{j}} + D^{(qq)}_{\mathbf{ij}}\partial_{q_\mathbf{i}}\partial_{q_\mathbf{j}}],$$

$$D^{(pp)}_{\mathbf{ij}} = \frac{1}{N}\sum_{\mathbf{k}} b^2_{\mathbf{k}}\alpha_{\mathbf{k}}\cos\mathbf{k}\cdot(\mathbf{i}-\mathbf{j}),$$

$$D^{(qq)}_{\mathbf{ij}} = \frac{1}{N}\sum_{\mathbf{k}} a^2_{\mathbf{k}}\alpha_{\mathbf{k}}\cos\mathbf{k}\cdot(\mathbf{i}-\mathbf{j}),$$

$$\alpha_{\mathbf{k}} = \frac{\hbar}{2\omega_{\mathbf{k}}}\mathcal{L}_{\mathbf{k}},$$

$$\mathcal{L}_{\mathbf{k}} = \coth f_{\mathbf{k}} - \frac{1}{f_{\mathbf{k}}},$$

$$f_{\mathbf{k}} = \frac{\beta\hbar\omega_{\mathbf{k}}}{2},$$

$$\omega_{\mathbf{k}} = a_{\mathbf{k}}b_{\mathbf{k}},$$

$$a^2_{\mathbf{k}} = \frac{1}{N}\sum_{\mathbf{ij}} e^{i\mathbf{k}\cdot(\mathbf{i}-\mathbf{j})}A^2_{\mathbf{ij}},$$

$$b^2_{\mathbf{k}} = \frac{1}{N}\sum_{\mathbf{ij}} e^{i\mathbf{k}\cdot(\mathbf{i}-\mathbf{j})}B^2_{\mathbf{ij}},$$

where $\mathbf{i}$ and $\mathbf{j}$ are sites on the lattice, while $A^2_{\mathbf{ij}}$ and $B^2_{\mathbf{ij}}$ are the LCA approximations of the fundamental renormalization parameters of the theory:

$$A^2_{\mathbf{ij}}(\boldsymbol{p},\boldsymbol{q}) \equiv \partial_{p_\mathbf{i}}\partial_{p_\mathbf{j}} e^{\Delta}\mathcal{H}(\boldsymbol{p},\boldsymbol{q}) \simeq A^2_{\mathbf{ij}},$$

$$B^2_{\mathbf{ij}}(\boldsymbol{p},\boldsymbol{q}) \equiv \partial_{q_\mathbf{i}}\partial_{q_\mathbf{j}} e^{\Delta}\mathcal{H}(\boldsymbol{p},\boldsymbol{q}) \simeq B^2_{\mathbf{ij}};$$

their dependence upon the phase-space coordinate $(\boldsymbol{p},\boldsymbol{q})$ is eliminated by the LCA.

As suggested in Ref. 11, and for the reasons given in Sec. III, in this work we define the specific LCA to be used, by setting $A^2_{\mathbf{ij}}(\boldsymbol{p},\boldsymbol{q}) \approx \langle A^2_{\mathbf{ij}}(\boldsymbol{p},\boldsymbol{q})\rangle^{\mathrm{SCHA}}_{\mathrm{eff}}$ [and similarly for $B^2_{\mathbf{ij}}(\boldsymbol{p},\boldsymbol{q})$], where $\langle\cdots\rangle^{\mathrm{SCHA}}_{\mathrm{eff}}$ is the SCHA approximation of the classical-like average $\langle\cdots\rangle_{\mathrm{eff}}$ with the effective Hamiltonian, Eq. (B8) below. We then have (see Ref. 11)

$$A^2_{\mathbf{ij}} = \langle \partial_{p_\mathbf{i}}\partial_{p_\mathbf{j}} e^{\Delta}\mathcal{H}(\boldsymbol{p},\boldsymbol{q})\rangle^{\mathrm{SCHA}}_{\mathrm{eff}},$$

$$B^2_{\mathbf{ij}} = \langle \partial_{q_\mathbf{i}}\partial_{q_\mathbf{j}} e^{\Delta}\mathcal{H}(\boldsymbol{p},\boldsymbol{q})\rangle^{\mathrm{SCHA}}_{\mathrm{eff}}.$$

Let us consider now the case of the spin Hamiltonian (1). We consider the lattice as subdivided into the usual AFM positive and negative sublattices and hereafter use the notation $(-)^{\mathbf{i}} = \pm 1$ for the site $\mathbf{i}$ belonging to the former or the latter, respectively. The Weyl symbol for $\hat{\mathcal{H}}$ (using the DM transformation) is given by[6]

$$\frac{\mathcal{H}}{J\widetilde{S}^2} = -\frac{1}{2}\sum_{\mathbf{i},\mathbf{d}}\Bigg[(1-z^2_\mathbf{i})(1-z^2_{\mathbf{i}+\mathbf{d}}) + \left(1-\frac{z^2_\mathbf{i}+z^2_{\mathbf{i}+\mathbf{d}}}{4}\right)(q_\mathbf{i}q_{\mathbf{i}+\mathbf{d}} - p_\mathbf{i}p_{\mathbf{i}+\mathbf{d}}) + i(-)^{\mathbf{i}}\frac{z^2_\mathbf{i}-z^2_{\mathbf{i}+\mathbf{d}}}{4}(q_\mathbf{i}p_{\mathbf{i}+\mathbf{d}} + p_\mathbf{i}q_{\mathbf{i}+\mathbf{d}})\Bigg], \tag{B2}$$

where $(p_\mathbf{i},q_\mathbf{i})$ are the Weyl symbols of canonical operators $(\hat{p}_\mathbf{i},\hat{q}_\mathbf{i})$ such that $[\hat{q}_\mathbf{i},\hat{p}_\mathbf{j}] = i\widetilde{S}^{-1}\delta_{\mathbf{ij}}$, and $z^2_\mathbf{i} \equiv (q^2_\mathbf{i}+p^2_\mathbf{i})/2$. It is simpler to use $J\widetilde{S}^2$ as the energy unit, i.e., to apply the above framework to the dimensionless Hamiltonian $\mathcal{H}(\boldsymbol{p},\boldsymbol{q})/J\widetilde{S}^2$, so that all the relevant quantities are dimensionless; in particular, $\beta \to 1/t$ and $\hbar \to 1/\widetilde{S}$.

The first step to close the self-consistent scheme described above is then the evaluation of $e^{\Delta}\mathcal{H}(\boldsymbol{p},\boldsymbol{q})$. By performing the transformation $\mathbf{k} \to (\pi,\pi) - \mathbf{k}$ one can establish the identity

$$D^{(qq)}_{\mathbf{i},\mathbf{i}+\mathbf{r}} = (-)^{r_1+r_2} D^{(pp)}_{\mathbf{i},\mathbf{i}+\mathbf{r}}, \tag{B3}$$

where $\mathbf{r} = (r_1,r_2)$; in particular, only the following two renormalization parameters appear in the effective Hamiltonian:

$$D \equiv D^{(qq)}_{\mathbf{ii}} = D^{(pp)}_{\mathbf{ii}},$$

$$D' \equiv D^{(qq)}_{\mathbf{i},\mathbf{i}+\mathbf{d}} = -D^{(pp)}_{\mathbf{i},\mathbf{i}+\mathbf{d}}, \tag{B4}$$

where $\mathbf{d} = (\pm 1,0)$ or $(0,\pm 1)$ is a nearest-neighbor displacement. We then find, for nearest neighbors $\mathbf{i}$ and $\mathbf{j} = \mathbf{i}+\mathbf{d}$,

$$e^{\Delta}z^2_\mathbf{i} = z^2_\mathbf{i} + D,$$

$$e^{\Delta}q_\mathbf{i}q_\mathbf{j} = q_\mathbf{i}q_\mathbf{j} + D',$$

$$e^{\Delta}p_\mathbf{i}p_\mathbf{j} = p_\mathbf{i}p_\mathbf{j} - D';$$

furthermore,

$$e^{\Delta}z^2_\mathbf{i}z^2_\mathbf{j} = z^2_\mathbf{i}z^2_\mathbf{j} + D(z^2_\mathbf{i}+z^2_\mathbf{j}) + D'(q_\mathbf{i}q_\mathbf{j} - p_\mathbf{i}p_\mathbf{j}) + D^2 + D'^2$$

and

$$e^{\Delta}(z^2_\mathbf{i}+z^2_\mathbf{j})(q_\mathbf{i}q_\mathbf{j} - p_\mathbf{i}p_\mathbf{j}) = (z^2_\mathbf{i}+z^2_\mathbf{j}+4D)(q_\mathbf{i}q_\mathbf{j} - p_\mathbf{i}p_\mathbf{j}) + 4D'(z^2_\mathbf{i}+z^2_\mathbf{j}) + 8DD',$$

$$e^{\Delta}(z^2_\mathbf{i}-z^2_\mathbf{j})(q_\mathbf{i}q_\mathbf{j} + p_\mathbf{i}p_\mathbf{j}) = (z^2_\mathbf{i}-z^2_\mathbf{j})(q_\mathbf{i}q_\mathbf{j} + p_\mathbf{i}p_\mathbf{j}).$$

It is important that the imaginary part of $\mathcal{H}(\boldsymbol{p},\boldsymbol{q})$ does not contribute any renormalization term: this in fact assures the final effective spin Hamiltonian, i.e., the one obtained after having performed the classical version of the inverse of the DM transformation on $\mathcal{H}_{\mathrm{eff}}(\boldsymbol{p},\boldsymbol{q})$, to be real. By defining $\theta^2 \equiv 1 - \mathcal{D}/2$ with $\mathcal{D} \equiv (D - D')$, we find

$$\frac{e^{\Delta}\mathcal{H}(\boldsymbol{p},\boldsymbol{q})}{J\widetilde{S}^2} = -\frac{1}{2}\sum_{\mathbf{i},\mathbf{d}}\Bigg[\theta^4 - \theta^2(z^2_\mathbf{i}+z^2_{\mathbf{i}+\mathbf{d}}) + z^2_\mathbf{i}z^2_{\mathbf{i}+\mathbf{d}} + \left(\theta^2 - \frac{z^2_\mathbf{i}+z^2_{\mathbf{i}+\mathbf{d}}}{4}\right)(q_\mathbf{i}q_{\mathbf{i}+\mathbf{d}} - p_\mathbf{i}p_{\mathbf{i}+\mathbf{d}}) + i(-)^{\mathbf{i}}\frac{z^2_\mathbf{i}-z^2_{\mathbf{i}+\mathbf{d}}}{4}(q_\mathbf{i}p_{\mathbf{i}+\mathbf{d}} + p_\mathbf{i}q_{\mathbf{i}+\mathbf{d}})\Bigg];$$

this is the only term of $\mathcal{H}_{\mathrm{eff}}(\boldsymbol{p},\boldsymbol{q})$ we need to determine $a^2_\mathbf{k}$ and $b^2_\mathbf{k}$ (as configuration-independent terms do not enter the evaluation of $\langle\cdots\rangle^{\mathrm{SCHA}}_{\mathrm{eff}}$), which are easily found to be

$$a^2_\mathbf{k} = 4\kappa^2(1+\gamma_\mathbf{k}),$$

$$b^2_\mathbf{k} = 4\kappa^2(1-\gamma_\mathbf{k}), \tag{B5}$$

where $\gamma_\mathbf{k} = (\cos k_1 + \cos k_2)/2$ and we introduced the SCHA renormalization parameter

$$\kappa^2 = 1 - \frac{1}{2N\widetilde{S}}\sum_\mathbf{k}(1-\gamma^2_\mathbf{k})^{1/2}\coth f_\mathbf{k}, \tag{B6}$$

that can also be written as in Eqs. (12). The renormalized frequencies $\omega_\mathbf{k}$ are hence given by Eqs. (12); the dimensionless parameter $f_\mathbf{k}$ can be written as $f_\mathbf{k} = \omega_\mathbf{k}/(2\widetilde{S}t)$. With the above determinations one can express $\mathcal{D}$ as in Eq. (9), and the procedure is completed by the self-consistent solution of Eqs. (12). As for the first uniform term appearing in Eq. (B1), one easily finds

$$\frac{1}{N}\sum_\mathbf{k}\omega^2_\mathbf{k}\alpha_\mathbf{k} = \frac{t}{N}\sum_\mathbf{k} f_\mathbf{k}\mathcal{L}_\mathbf{k} = 2\kappa^2\mathcal{D}. \tag{B7}$$

To recast $e^{\Delta}\mathcal{H}(\boldsymbol{p},\boldsymbol{q})$ in the form of a spin Hamiltonian, we scale $(\boldsymbol{p},\boldsymbol{q}) \to (\theta\boldsymbol{p},\theta\boldsymbol{q})$ so that

$$\frac{e^{\Delta}\mathcal{H}(\boldsymbol{p},\boldsymbol{q})}{J\widetilde{S}^2} = \frac{\theta^4}{2}\sum_{\mathbf{i},\mathbf{d}}\Bigg[(1-z^2_\mathbf{i})(1-z^2_{\mathbf{i}+\mathbf{d}}) + \left(1-\frac{z^2_\mathbf{i}+z^2_{\mathbf{i}+\mathbf{d}}}{4}\right)(q_\mathbf{i}q_{\mathbf{i}+\mathbf{d}} - p_\mathbf{i}p_{\mathbf{i}+\mathbf{d}}) + i(-)^{\mathbf{i}}\frac{z^2_\mathbf{i}-z^2_{\mathbf{i}+\mathbf{d}}}{4}(q_\mathbf{i}p_{\mathbf{i}+\mathbf{d}} + p_\mathbf{i}q_{\mathbf{i}+\mathbf{d}})\Bigg];$$

this equation has the same functional form of the Weyl symbol for the Hamiltonian, Eq. (B2), so that performing the

inverse of the classical DM transformation we eventually find the form reported in Eq. (6), where the change in the phase-space measure by the factor θ^{2N} due to the above scaling is absorbed in the effective Hamiltonian as an additive logarithmic term, $-Nt\ln\theta^2$.

Finally, the PQSCHA expresses the general thermal average of an observable $\hat{\mathcal{O}}(\hat{\boldsymbol{p}},\hat{\boldsymbol{q}})$ as the classical-like average with the effective Hamiltonian

$$\langle\hat{\mathcal{O}}\rangle=\frac{1}{\mathcal{Z}}\int\frac{d\boldsymbol{p}d\boldsymbol{q}}{(2\pi)^N}\widetilde{\mathcal{O}}(\boldsymbol{p},\boldsymbol{q})e^{-\beta\mathcal{H}_{\rm eff}(\boldsymbol{p},\boldsymbol{q})}\equiv\langle\widetilde{\mathcal{O}}\rangle_{\rm eff}, \quad \text{(B8)}$$

of the phase-space function

$$\widetilde{\mathcal{O}}(\boldsymbol{p},\boldsymbol{q})\equiv e^{\Delta}\mathcal{O}(\boldsymbol{p},\boldsymbol{q}), \quad \text{(B9)}$$

where $\mathcal{O}(\boldsymbol{p},\boldsymbol{q})$ is the Weyl symbol of the operator $\hat{\mathcal{O}}$. In terms of the classical spin variables Eq. (B8) becomes just Eq. (15). In the case of the correlation functions $G(\mathbf{r})=\langle\hat{\boldsymbol{S}}_{\mathbf{i}}\cdot\hat{\boldsymbol{S}}_{\mathbf{i}+\mathbf{r}}\rangle$ the procedure leading to the Weyl symbol $S_{\mathbf{i},\mathbf{i}+\mathbf{r}}(\boldsymbol{p},\boldsymbol{q})$ of the operator $\hat{\boldsymbol{S}}_{\mathbf{i}}\cdot\hat{\boldsymbol{S}}_{\mathbf{i}+\mathbf{r}}$ and hence to the expression of $e^{\Delta}S_{\mathbf{i},\mathbf{i}+\mathbf{r}}(\boldsymbol{p},\boldsymbol{q})$ is obviously analogous to the one described for the Hamiltonian, and the final result is easily found to be as reported in Eq. (17).

*Electronic address: cuccoli@fi.infn.it
†Electronic address: tognetti@fi.infn.it
‡Electronic address: vaia@ieq.fi.cnr.it
§ Present address: Istituto di Elettronica Quantistica - C.N.R., via Panciatichi 56/30, I-50127 Firenze, Italy. Electronic address: verrucchi@ieq.fi.cnr.it

[1] A. Sokol and D. Pines, Phys. Rev. Lett. **71**, 2813 (1993).
[2] S. Chakravarty, in *High Temperature Superconductivity*, edited by K. S. Bedell *et al.* (Addison Wesley, New York, 1990).
[3] N. D. Mermin and H. Wagner, Phys. Rev. Lett. **17**, 1133 (1966).
[4] E. J. Neves and J. F. Perez, Phys. Lett. **114A**, 331 (1986).
[5] E. Manousakis, Rev. Mod. Phys. **63**, 13 (1991).
[6] A. Cuccoli, V. Tognetti, P. Verruchi, and R. Vaia, Phys. Rev. Lett. **77**, 3439 (1996).
[7] F. D. M. Haldane, Phys. Rev. Lett. **50**, 1153 (1983); I. Affleck, Nucl. Phys. B **257**, 397 (1985).
[8] S. Chakravarty, B. I. Halperin, and D. R. Nelson, Phys. Rev. B **39**, 2344 (1989).
[9] P. Hasenfratz and F. Niedermayer, Phys. Lett. B **268**, 231 (1991).
[10] N. Elstner *et al.*, Phys. Rev. Lett. **75**, 938 (1995); N. Elstner, Int. J. Mod. Phys. B **11**, 1753 (1997).
[11] A. Cuccoli, V. Tognetti, P. Verrucchi, and R. Vaia, Phys. Rev. A **45**, 8418 (1992).
[12] M. Greven *et al.*, Phys. Rev. Lett. **72**, 1096 (1994); M. Greven *et al.*, Z. Phys. B **96**, 465 (1995).
[13] K. Nakajima *et al.*, Z. Phys. B **96**, 479 (1995).
[14] P. Carretta, A. Rigamonti, and R. Sala, Phys. Rev. B **55**, 3734 (1997).
[15] R. J. Birgeneau *et al.*, J. Phys. Chem. Solids **56**, 1913 (1995).
[16] S. H. Shenker and J. Tobochnik, Phys. Rev. B **22**, 4462 (1980).
[17] J.-K. Kim, Phys. Rev. D **50**, 4663 (1994).
[18] M. S. Makivić and H.-Q. Ding, Phys. Rev. B **43**, 3562 (1991).
[19] J.-K. Kim, D. P. Landau, and M. Troyer, Phys. Rev. Lett. **79**, 1583 (1997); (private communication).
[20] M. Takahashi, Phys. Rev. B **40**, 2494 (1989).
[21] A. V. Chubukov, S. Sachdev, and J. Ye, Phys. Rev. B **49**, 11 919 (1994).
[22] B. Keimer *et al.*, Phys. Rev. B **46**, 14 034 (1992).
[23] A. Cuccoli, R. Giachetti, V. Tognetti, R. Vaia, and P. Verrucchi, J. Phys. Condens. Matter **7**, 7891 (1995).
[24] H.-W. Lee, Phys. Rep. **259**, 147 (1995).
[25] A. Cuccoli, V. Tognetti, P. Verrucchi, and R. Vaia, Phys. Rev. B **46**, 11 601 (1992).
[26] F. A. Berezin, Usp. Fiz. Nauk. **132**, 497 (1980) [Sov. Phys. Usp. **23**, 763 (1980)].
[27] F. Holstein and H. Primakoff, Phys. Rev. **58**, 1048 (1940).
[28] F. J. Dyson, Phys. Rev. **102**, 1217 (1956); S. V. Maleev, Zh. Eksp. Teor. Fiz. **33**, 1010 (1957).
[29] P. Carretta *et al.*, Il Nuovo Cimento **190**, 1193 (1997).
[30] A. Cuccoli, V. Tognetti, and R. Vaia, Phys. Rev. B **52**, 10 221 (1995).
[31] A. Cuccoli, V. Tognetti, R. Vaia, and P. Verrucchi, Phys. Rev. Lett. **79**, 1584 (1997).
[32] E. Brézin and J. Zinn-Justin, Phys. Rev. B **14**, 3110 (1976).
[33] B. J. Suh *et al.*, Phys. Rev. Lett. **75**, 2212 (1995).
[34] A. V. Chubukov, S. Sachdev, and J. Ye, Phys. Rev. B **49**, 11 919 (1994).